Appl. Phys. B 59, 649–653 (1994)

Applied Physics B Lasers and Optics

Superradiating $4P$–$4S$–$3P$ cascade of sodium vapour arising on the leading edge of the exciting laser pulse

Z. Kuprionis, V. Švedas

The Institute of Physics, Savanoriu Ave. 231, 2028 Vilnius, Lithuania
(Fax: +37-02/617-070, E-mail: VIKTORAS.VAICIKAUSKAS@nol.fi.lt)

Received in revised form 21 April 1994/Accepted 27 April 1994

Abstract. Investigations of the superradiating cascade of sodium vapour $4P$–$4S$–$3P$ ($\lambda_1 = 2.21$ μm and $\lambda_2 = 1.14$ μm) arising on the leading edge of the exciting laser pulse were carried out. The dependences of the actual delay time τ_D' of the λ_1 pulse on the population rise time of the laser-excited $4P$ state were measured and compared with those calculated following the existing theoretical model. The dependence of the actual delay time τ_D' on the inverse density of excited atoms $1/N^*$ is also presented. Analysis of this dependence revealed the influence of the Doppler dephasing and of the second, λ_2, transition on the formation of the λ_1 superradiance.

PACS: 32.50.+d, 42.50.+q

The generation of coherent pulses, based on the superradiance (SR) of atoms or molecules, shows some advantages over other methods of generation. The excited atoms and molecules are able to generate radiation without resonators in a wide spectral range, i.e., from FIR [1] to X-rays [2], and the superradiant pulse's shortness has no strict limits associated with the spectral width of the transition [1].

An excitation of the superradiating particles in most of the works is considered to be instantaneous. Finite duration of the excitation, in reality, influences the parameters of SR. At a sufficient density of radiating particles the SR pulse even merges in time with the laser pulse [3–5]. In this situation SR develops entirely during the laser excitation or, in other words, within the laser pulse. This "inner" SR is useful for the generation of short pulses, since the emitted SR pulse is shorter than the excitation pulse.

SR developing during laser excitation was found in the first experiment with an atomic SR [3]. The authors presumed the phase correlations to be washed out by regenerative laser pumping and the developing coherent pulses to be not of superradiant origin. Later works confirmed superradiant properties of the inner coherent pulses. About 1ns long visible SR pulses [6, 7], including those emitted in the resonance line of the atom [6], were investigated. A sequence of about 5 ns long SR pulses was observed within the 50 ns long excitation pulse [8]. The recent investigations in this field revealed the two-photon fluctuations of the inner SR pulse in the FIR range [5].

Formation of the short SR pulse of high energy under conditions when the population of a pumped level grows over the finite time τ was analysed in terms of coupled Maxwell-Schrödinger equations by MacGillivray and Feld [9]. In this case, the actual delay time τ_D', measured from the start of pumping, is longer than the ordinary delay time τ_D, which comes out in the case of an instantaneous excitation. The analytical generalization of a numerical solution of equations for the delay time can be written as [9]:

$$\tau_D' = \tau_D + \tau f(\tau), \tag{1}$$

where $f(\tau)$ is a weight function. If the population of the excited level $N^*(t)$ grows proportionally to the exponential function $A t^\beta$, where A is constant and $\beta > 0$, then

$$f = 1 - 1/(\beta + 1). \tag{2}$$

It is necessary to emphasize that the population rise time τ contributes to the delay time τ_D' not additively, but with the factor $f(\tau)$, and the (1) is more than the ordinary shift of the SR pulse on τ. Dependence (1) is not checked experimentally and the limits of its validity are not detailed in [9]. It is considered only that (1) is valid if $N^*(t)$ reaches a constant value before the SR pulse is emitted, i.e., $\tau < \tau_D'$.

Analysis of the formation of the SR pulse during the laser excitation and verification of (1) by variation of the population rise time τ are the goals of this work. The superradiance of sodium atoms occurring within a laser pulse was investigated in our previous works [10, 11]. The threshold properties [10], the polarization of SR [11], the competition of the transitions [10, 11] in Λ- and V-type branchings have been studied. In the present

article we investigate the sodium atom $4P$–$4S$–$3P$ SR cascade, arising on the leading edge of the exciting laser pulse, and analyse the interaction of the cascade transitions.

1 Experimental setup and method

The experimental arrangement is similar to that of our previous works [10, 11]. The sodium atoms were excited from the ground $3S_{1/2}$ state to the $4P_{3/2}$ state by the second harmonic of a dye laser ($\lambda = 330.2$ nm). The laser pulse comprising about ten longitudinal modes of the dye oscillator had a spectral width of 0.002 nm and a duration $\tau_p = 10$ ns. The excitation pulse was focused into the $L = 4$ cm long sodium-vapour cell, forming a cylinder of excited atoms with the cross-sectional area $S = 6 \times 10^{-3}$ cm^2. The superradiance on the $4P$–$4S$ ($\lambda_1 = 2.21$ μm) and $4S$–$3P$ ($\lambda_2 = 1.14$ μm) transitions was investigated. Sodium atoms excited to the $4P$ state superradiate also in the $4P$–$3D$–$3P$ branch. We have registered the $3D$–$3P$ SR pulses, the energy of which was more than hundred-fold less than that of the $4S$–$3P$ SR pulses in the dominating $4P$–$4S$–$3P$ branch [11]. Thus, SR in the $4P$–$3D$–$3P$ branch can, to a good approximation, be neglected.

The atomic vapour density N was varied in the range 10^{11}–10^{13} cm^{-3} [14]. It was determined from the temperature T of the coldest spot of the cell's side-arm, where the metallic sodium was placed. T was varied in the interval 430–500 K.

The wavelengths of the forward SR were selected by adequate filters. The pulses were monitored by a GaInAsSb photodiode (with 1 ns time resolution) and by a Ge avalanche photodiode (with 0.3 ns time resolution), respectively, for the λ_1 and λ_2 SR pulses. The SR pulses were averaged by a sampling-oscillograph and plotted by a chart recorder.

We considered the preparation of the $4P$ state in detail. In further calculations the exciting laser pulse was substituted by the same area triangle-shaped pulse. Crossing point of the leading edge of this triangle-shaped pulse with the time axis was taken as the start of the time scale (solid arrow in Fig. 1). The apex of this triangle coincides in time with the laser pulse maximum. On the leading edge of the exciting pulse the excited-state density N^* grows like $N\Lambda t^2$ (N is the atomic vapour density). The coefficient

$$\Lambda = E\sigma R/S\tau_p \varepsilon t_m, \tag{3}$$

where E is the energy of the laser pulse, ε is the energy of the laser photon, σ is the absorption cross-section of the $3S_{1/2}$–$4P_{3/2}$ transition, R is the excitation spectral ratio (the ratio of the transition width to the laser linewidth) and t_m is the temporal position of the laser pulse's maximum.

The saturation condition $N^* = 2/3\ N$ for the $3S_{1/2}$–$4P_{3/2}$ transition is reached within the time τ, that means $\Lambda\tau^2 = 2/3$. According to this relation and (3), the population rise time, which is equal to the saturation time in our case, is

$$\tau = (2S\tau_p \varepsilon t_m/3E\sigma R)^{1/2}. \tag{4}$$

For a linear leading edge, the parameter β of (2) equals 2, and the actual delay is

$$\tau_D' = \tau_D + \frac{2}{3}\tau,$$

or

$$\tau_D' = \tau_D + \frac{2}{3}(2S\tau_p \varepsilon t_m/3E\sigma R)^{1/2}, \tag{5}$$

in our situation. The laser pulse reaches its maximum at $t_m = 4.6$ ns. The excitation spectral ratio $R = 0.4$ is determined from the measurements of the laser pulse absorption on the $3S_{1/2}$–$4P_{3/2}$ transition. The absorption cross section $\sigma = 8.7 \times 10^{-14}$ cm^2 is calculated according to [12] by substituting the Doppler shape of the line by a rectangle of the same height and area, and assuming the oscillator strength to be equal 0.010 [13].

Summarizing the analysis of the excited state preparation one can conclude that τ_D' consists of two independent parts: τ_D, which depends on N^*, and an other one, that depends on E. In our measurements N^* was varied by alteration of the vapour density N, and E was decreased by a set of attenuating filters.

To compare the experimental τ_D' as a function of N^* with theory, we made use of [15], where the dephasing process was taken into account. We will show below that the dephasing could not be omitted in the analysis of the results. According to [15] the ordinary delay time is

$$\tau_D = \frac{L}{c}\left(\frac{1}{2} + \left\{\left(\frac{G}{2\alpha}\right)^{1/2} - \left[\frac{G}{2\alpha} - \frac{1}{2\alpha}\ln\left(2\pi N^* V\right)\right]^{1/2}\right\}^2\right), \tag{6}$$

where c is the speed of light, $\alpha = L/(2cT_2')$ is the dephasing parameter, $G = 2T_2'/\tau_R$ is the field gain, T_2' is the dephasing time, $1/T_2' = \Gamma + \Delta$, Γ and Δ are the homogeneous and inhomogeneous linewidths, respectively, $\tau_R = 8\pi/(AN^*\lambda^2 L)$ is the characteristic superradiance time, A is the transition probability and $V = SL$ is the volume of the excited vapour.

In our situation Γ is the natural linewidth of the $4P$–$4S$ transition ($\Gamma = 3.26 \times 10^7$ s^{-1} [13]), Δ is the inverse of the Doppler dephasing time $T_2^* = 1.1$ ns [3] and $A = 6.58 \times 10^6$ s^{-1} [13]. Because of the inaccuracies [17] of the transition probability A and the uncertainty of the vapour density N [14] we have used in the calculations the fitting factor for the gain $G (G \propto AN^*)$.

In general, τ_D is a nonlinear function of $1/N^*$, and only at large gain, $G \gg \ln(2\pi N^* V)$, the linearity is valid. Then,

$$\tau_D = \frac{L}{c}\left[\frac{1}{2} + \frac{1}{8G\alpha}\ln^2\left(2\pi N^* V\right)\right], \tag{6a}$$

where $G\alpha$ varies as N^*. In (6a) the delay does not contain any dephasing time. The majority of experimental works assume τ_D to be proportional to $1/N^*$. A different treatment of $\tau_D(N^*)$ is found in [16], where the investigation

of the KCl:O_2^- cooperative emission at cryogenic temperatures was carried out.

2 Results and discussions

The plot of the λ_1 and λ_2 SR pulses for several vapour densities is given in Fig. 1. Every pulse trace in Fig. 1 is an average of about thousand pulses. The dependences of the actual delay τ_D' of the λ_1 pulse on the pulse energy E are shown in Fig. 2. Although the laser saturates the $3S_{1/2}$–$4P_{3/2}$ transition for all energy values of Fig. 2, due to the dependence of the saturation time τ on E, τ_D', increases when E decreases. The lines in Fig. 2 indicate τ_D', calculated according to (5) and (6). The value of the fitting factor for G that equals 1.6 was obtained on the basis of data points of Fig. 4 (see later). The same value of this factor corresponds to the data points of Fig. 2, while $\tau_D' \lessapprox 5$ ns. Agreement of experimental and calculated τ_D' means that for the specified conditions of (4) the dependence of saturation time τ on E is

$$\tau = 1.6 \text{ ns } (E_o/E)^{1/2}, \tag{7}$$

where $E_o = 1.3$ μJ. This time is plotted on Fig. 2 as the second abscissa. When the actual delay τ_D' exceeds about 5 ns (N^* becomes smaller than about 3×10^{11} cm^{-3}), it increases more rapidly than $E^{-1/2}$. This deviation of the delay τ_D' from (5) requires further investigation and more sophisticated models of SR arising during the laser excitation. Evidently, the fast decrease of the amplitude of the pulse trace (Fig. 3), occurring at laser energies $E \lessapprox E_o/4$, has the same origin as the rapid increase of τ_D'. The dependence of the delays τ_D' of the λ_1 and λ_2 pulses on the density of the excited atoms N^* are shown in Fig. 4. At atomic densities N^* smaller than about 10^{12} cm^{-3}, only the λ_1 SR pulse was emitted. This observation enables us to use (6), which is deduced for the two-level superradiance, and to compare the experimental delay τ_D' with theory. The experimental delay of the λ_1 pulse and the delay calculated according to (5) and (6) (solid line in Fig. 4) agree very well. It is necessary to show the sensitivity of the calculated dependence in Fig. 4 to the field gain G. The shape of this curve and its crossing point with the ordinate axis do not change when G varies, but the slope of the curve does. Variation of the above-mentioned fitting factor 1.6 by ±0.1 causes a variation of the largest delay of 8.7 ns (Fig. 4) by (−0.8, +1.0) ns.

The dependence of τ_D' on $1/N^*$ is nonlinear, τ_D' increases faster than $1/N^*$ at $N^* \lessapprox 4 \times 10^{11}$ cm^{-3}. Searching for the reasons of this nonlinearity we have omitted the Doppler dephasing in the calculations. The delay τ_D' turns out several nanoseconds smaller in the range of small densities (broken line of Fig. 4), and its dependence on $1/N^*$ is close to linear. Thus, we suppose that the deviation from linearity for the λ_1 pulse is caused by Doppler dephasing. The delay of the second pulse of the $4P$–$4S$–$3P$ cascade at λ_2 is also a nonlinear function of $1/N^*$ (Fig. 4); it increases faster than $1/N^*$ at $N^* \lessapprox 10^{12}$ cm^{-3}.

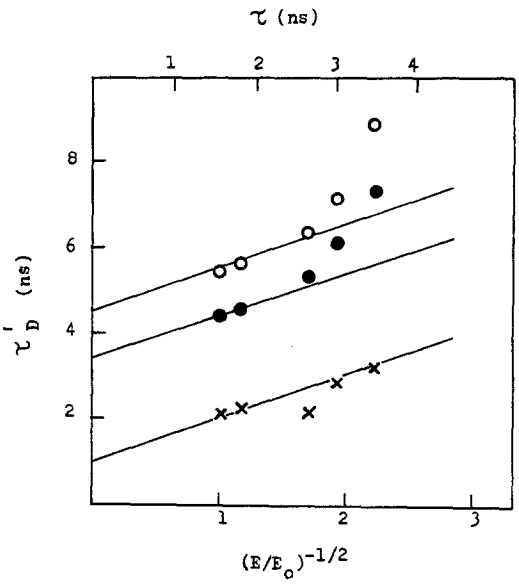

Fig. 2. Actual delay time τ_D' of the $\lambda_1 = 2.21$ μm SR pulse vs laser pulse energy E. The densities of vapour are 1.8×10^{12} cm^{-3} (x), 5.8×10^{11} cm^{-3} (●) and 4.7×10^{11} cm^{-3} (○). $E_o = 1.3$ μJ. The *lines* show the delay time, calculated according to (5, 6). The additional abscissa is the saturation time of the $3S_{1/2}$–$4P_{3/2}$ transition

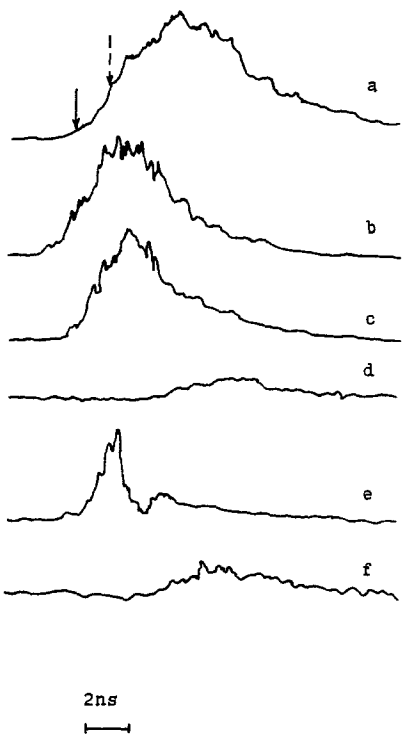

Fig. 1a–f. The plots of the excitation pulse (**a**), the $4P$–$4S$ SR pulses (**b, c, d**) and the $4S$–$3P$ SR pulses (**e, f**) (amplitudes are not to scale). The densities of atomic vapour are as follows: 8.3×10^{12} cm^{-3} (**b, e**), 1.2×10^{12} cm^{-3} (**c, f**) and 3.3×10^{11} cm^{-3} (**d**). The marks are the start of the time reading *(solid arrow)* and the saturation time of the $3S_{1/2}$–$4P_{3/2}$ transition at a laser pulse energy of 1.3 μJ *(broken arrow)*

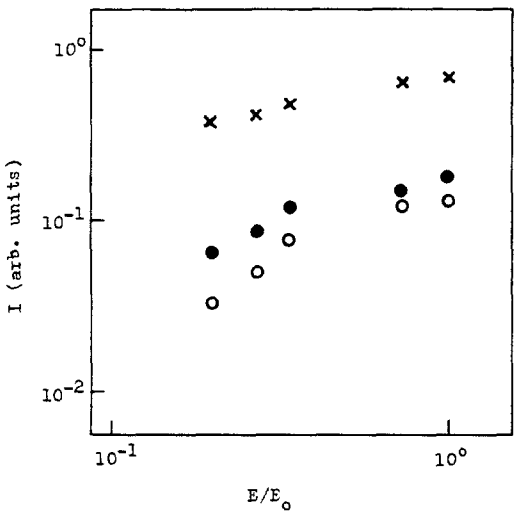

Fig. 3. The amplitudes I of the λ_1 SR pulse traces vs E. The symbols and parameters are as in Fig. 2

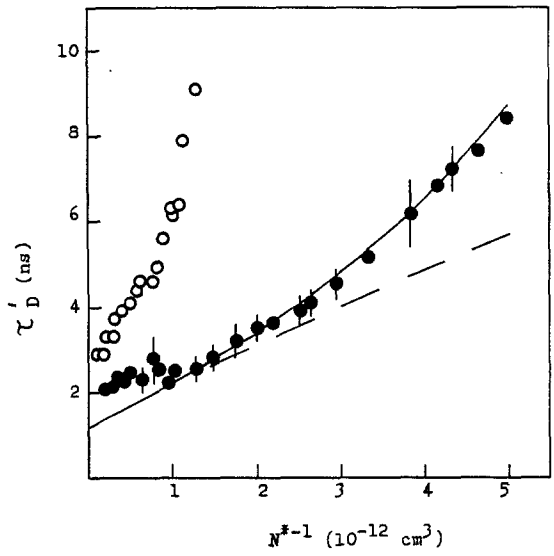

Fig. 4. Dependences on N^* of the actual delay τ'_D of the $\lambda_1 = 2.21$ μm (●) and $\lambda_2 = 1.14$ μm (○) SR pulses at the laser pulse energy of 1.3 μJ. In the calculations of τ'_D the Doppler dephasing time was $T_2^* = 1.1$ ns *(solid line)* and $T_2^* = \infty$ *(broken line)*

At $N^* \gtrapprox 10^{12}$ cm^{-3} the delay of the λ_1 pulse differs from that marked by the solid line. We have interpreted this difference by the influence of the λ_2 SR pulse in the two-transition $4P$–$4S$–$3P$ cascade. A two-transition cascade is analysed theoretically in [18]. If the transition probability of the second cascade transition is larger than that of the first transition, the SR of the second transition, according to [18], is finishing faster than that of the first transition. The second transition has emptied the energy level that is common to both transitions of the cascade. Since the SR rate depends on the product of populations of pairs of the levels involved [19], the SR of the first transition is interrupted, and part of the population of the highest level in the cascade remains "trapped" and does not contribute to the SR pulse [18]. The transition probability of the λ_2 pulse in the sodium atom is larger than that of the λ_1 pulse ($A_{4S-3P}/A_{4P-4S} = 3.93$ [13]). Therefore, "trapping" of $4P$ level population is possible at $N^* \gtrapprox 10^{12}$ cm^{-3} when the λ_2 SR occurs. The density of atoms contributing to the λ_1 SR can, in this situation, be smaller than N^*, and the measured delay τ'_D (Fig. 4) is larger than that calculated according to (5) and (6).

Interaction of the superradiating transitions reveals itself not only in cascades, but also in transitions with a

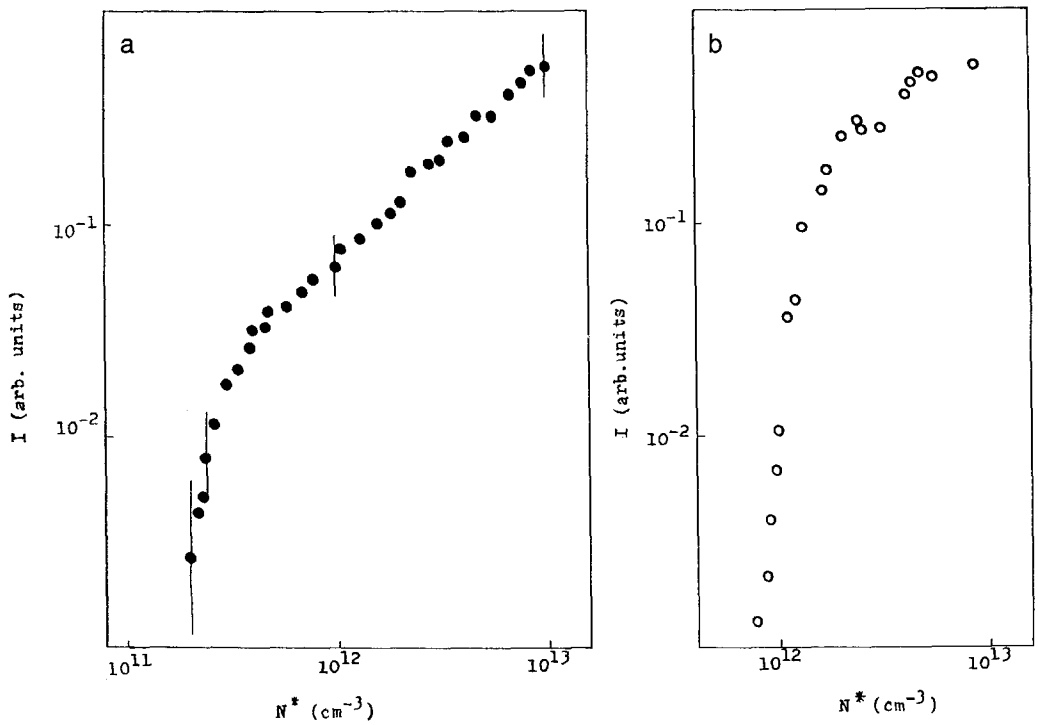

Fig. 5a, b. Amplitudes I of traces of the λ_1 (**a**) and λ_2 (**b**) SR pulses vs density of the excited atoms N^*

common upper level (Λ-type branching) or lower level (V-type branching) [19]. As in cascades, in Λ-type branching the faster transition suppresses the slower one [19]. We observed this suppression in competition of fine structure components of the sodium $4S$–$3P$ transition [11]. The energy of the $4S_{1/2}$–$3P_{3/2}$ SR pulse ($\lambda=1.140$ μm) was 20 times the energy of the $4S_{1/2}$–$3P_{1/2}$ pulse ($\lambda=1.138$ μm), whereas the ratio of transition probabilities of the fine structure components is 2. Obviously, the $4S_{1/2}$–$3P_{3/2}$ component quenches the $4S_{1/2}$–$3P_{1/2}$ one.

The dependence of the amplitudes of traces of the λ_1 and λ_2 pulses on N^* are given in Fig. 5. The SR pulses of both wavelengths rise fast at the threshold, $N^*_{th} \approx 2\times10^{11}$ cm^{-3} for the λ_1 pulse and $N^*_{th} \approx 8\times10^{11}$ cm^{-3} for the λ_2 one, and then increase linearly with N^*. By using a calibrated pyroelectric detector, we also measured a ratio of the emitted SR quanta and of the number of the excited atoms, i.e., the quantum efficiency of the transition. The efficiency of the λ_1 SR pulse amounted to about 10% in the linear part of $I(N^*)$.

3 Conclusions

The development of sodium vapour $4P$–$4S$ ($\lambda_1=2.21$ μm) SR pulses on the leading edge of laser pulse was investigated. While the second transition ($4S$–$3P$, $\lambda_2=1.14$ μm) of the cascade not arises ($N^* \lessapprox 10^{12}$ cm^{-3}), the actual delay τ_D' of the λ_1 pulse mainly obeys relation (5). The dependences of τ_D' on E deviates from (5) when $E \lessapprox E_o/4$ (E_o is the largest exciting pulse energy) and $N^* \lessapprox 3\times10^{11}$ cm^{-3}. This deviation requires further investigation. At $N^* \gtrapprox 10^{12}$ cm^{-3} ($E=E_o$) an influence of the λ_2 SR on the λ_1 SR pulse evidently occurs.

When $N^* \lessapprox 5\times10^{11}$ cm^{-3} ($E=E_o$) τ_D' is a nonlinear function of $1/N^*$. The Doppler dephasing was explained to be the reason for this nonlinearity.

Acknowledgements. This work was supported, in part, by a Meyer Foundation Grant awarded by the American Physical Society.

References

1. D.P. Scherrer, A.W. Kälin, R. Kesselring, F.K. Kneubühl: Appl. Phys. B **52,** 250 (1991)
2. J.C. MacGillivray, M.S. Feld: Appl. Phys. Lett. **31,** 74 (1977)
3. M. Gross, C. Fabre, P. Pillet, S. Haroche: Phys. Rev. Lett. **36,** 1035 (1976)
4. V. Švedas, Z. Kuprionis: Appl. Phys. B **52,** 385 (1991)
5. J.S. Bakos, D.P. Scherrer, F.K. Kneubühl: Phys. Rev. A **46,** 410 (1992)
6. C. Brechignac, Ph. Cahuzac: J. Phys. B **14,** 221 (1981)
7. Ph. Cahuzac, H. Sontag, P.E. Toschek: Opt. Commun. **31,** 37 (1979)
8. A. Crubellier, S. Liberman, D. Mayou, P. Pillet, M.G. Schweighofer: Opt. Lett. **7,** 16 (1982)
9. J.C. MacGillivray, M.S. Feld: Phys. Rev. A **23,** 1334 (1981)
10. Z. Kuprionis, V. Švedas: Litov. Fiz. Sb. **28,** 763 (1988) (in Russian)
11. Z. Kuprionis, V. Švedas: Litov. Fiz. Sb. **29,** 583 (1989) (in Russian)
12. I.I. Sobel'man: *Introduction to the Theory of Atomic Spectra* (Pergamon, New York 1972)
13. E.M. Anderson, V.A. Zilitis: Opt. Spektrosk. **16,** 177 (1964) (in Russian)
14. R.E. Hohig: RCA Rev. **23,** 567 (1962)
15. A.V. Andreyev: Usp. Fiz. Nauk **160,** 1 (1990) (in Russian)
16. M.M. Malcuit, J.J. Maki, D.J. Simkin, R.W. Boyd: Phys. Rev. Lett. **59,** 1189 (1987)
17. M.C.E. Huber, R.J. Sandeman: Phys. Scr. **22,** 373 (1980)
18. W.A. Molander, C.R. Stroud, Jr.: J. Phys. B **15,** 2109 (1982)
19. A. Crubellier, M.G. Schweighofer: Phys. Rev. A **16,** 1797 (1978)